

EVALUATING THE INDIAN AND PACIFIC TSUNAMIS REMOTE IMPACTS IN THE GULF OF GUINEA

Elisée TOUALY^{1,2}, Alpha TOURE³, Nicholas Loukou KOUAME³,
et Angora AMAN¹

¹ *Climate Tropical Team, LASMES, Université Félix Houphouët Boigny, Abidjan, Côte d'Ivoire*

² *School of Science, Engineering, Technology and Mathematics (STEM), International University of Grand Bassam, Côte d'Ivoire*

³ *Equipe de Recherche Géophysique Appliquée, Laboratoire de Géologie Ressources Minérales et Energétiques, Université Félix Houphouët Boigny (LGRME), Abidjan, Côte d'Ivoire*

(reçu le 21 Juillet 2021 ; accepté le 02 Novembre 2021)

* Correspondance, e-mail : elisee.toualy@gmail.com

ABSTRACT

The Gulf of Guinea (GG) is located in the Atlantic Ocean between the Indian and Pacific Oceans where most of the tsunamis occur. With the global warming increasing the strength and the occurrence of natural events such as the El Niño, the earthquakes and the tsunamis, the bordering countries of the GG are now wondering about the remote impact of these events and particularly those of the tsunamis along their coasts. This study uses GLOSS sea level data from Indonesia, Japan, Ghana and Cameroon to determine the remote impact of tsunamis in the GG. This study showed that the 2004 Sumatra tsunami signal is observed at Ghana and Indonesia in the same respective frequency ranges of 0.008cpm (2 h) and 0.01cpm (1h40 mn), and of 0.016cpm (1 h) and 0.018 cpm (55 min) with, the variance greater in the Indian Ocean. The Fukushima tsunami reached also the GG in the frequency ranges similar to those of the Sumatra tsunami. The signals of these tsunamis travel during more than 24 hours before reaching the GG coastline where they induce a rise of the sea level less than 10mm. The time sampling of the data used that doesn't allow determining efficiently the peak energy and the tsunami wave heights. This sustains the need of equipment along the GG coastline to improve the data quality.

Keywords : *Tsunamis, Gulf of Guinea, spectral analysis, power spectrum, wavelet, data filter, Indian Ocean, Pacific Ocean, Atlantic Ocean.*

RÉSUMÉ

Estimation de l'impact des tsunamis des océans Indien et Pacifique dans le Golfe de Guinée

Le Golfe de Guinée (GG) se trouve dans l'océan Atlantique entre les océans Indiens et Pacifique. Les océans Indien et Pacifique sont les zones d'occurrence des tsunamis marins. Avec le réchauffement climatique accroissant l'intensité et les occurrences des phénomènes naturels tels que El Niño, les tremblements de terre et les tsunamis, les pays côtiers du GG s'inquiètent de plus en plus des impacts éloignés de ces phénomènes, particulièrement ceux des tsunamis. Cette étude utilise les données du niveau de la mer des stations GLOSS de l'Indonésie, du Japon, du Ghana et du Cameroun en vue de déterminer l'impact des tsunamis dans le GG. Cette étude a montré que le signal du tsunami de l'Indonésie est observé dans le GG dans la bande de fréquence 0.008cpm (2 h) et 0.01cpm (1 h 40 mn) et, dans la bande de fréquences 0.016 cpm (1 h) et 0.018 cpm (55 min) avec, une énergie plus grande dans l'océan Indien. Le signal du tsunami de Fukushima est aussi observé dans le GG dans les bandes de fréquences similaires à celles du tsunami de Sumatra. Le signal de ces tsunamis se propagent pendant environ 1 jour pour atteindre le GG où il entraîne une élévation du niveau de la mer inférieure à 10mm. Les données horaires utilisées ne permettent pas d'estimer efficacement la puissance spectrale et la hauteur des vagues des tsunamis dans le GG. Cette étude montre l'importance d'équiper les zones côtières du GG en instruments de mesure.

Mots-clés : *tsunamis, Golfe de Guinée, analyse spectral, puissance spectrale, analyse en ondelettes, filtrage de données, océan Indien, océan Pacifique.*

I - INTRODUCTION

The Gulf of Guinea (GG) is located in the Atlantic Ocean between 20°W and its Western coast and from the equator to the northern coast (**Figure 1**). It is a poor area with an economy still dependent of non-mechanical agriculture. Most of the infrastructures such as industries, airports and capitals of the coastal countries in the GG lays along the coast (**Figure 2**). Besides, these coastal zones concentrate about 31 % of the population and the main infrastructures. This coastal area is vulnerable because of being exposed to a variety of natural and potentially damaging events and also to an increasing rate of population [1]. The low-lying coastal areas of West Africa such as Abidjan, Cotonou and Lagos, are particularly exposed to sea-level rise and strong flooding during the passage of the West African Monsoon. In these

cities, more than 3,000,000 of people are exposed to climate change and extreme event impacts [1]. Extreme events have frequently occurred during these last decades and have often induced a severe coastline retreat and human life and infrastructures losses. The few studies focusing on these recent events have shown that there are due to swells generated since the low depression area North of the coast of South Africa [2] while the wave run-up is the major is the major forcing responsible for the extreme coastal flooding events [3]. Only one study has focused on the remote impact of 2004 Sumatra tsunami in the GG [4], therefore the question about the remote impact of the tsunami in the GG remains opened and constitutes a major concern for the different countries of the GG. This question constitutes the main objective of this study.

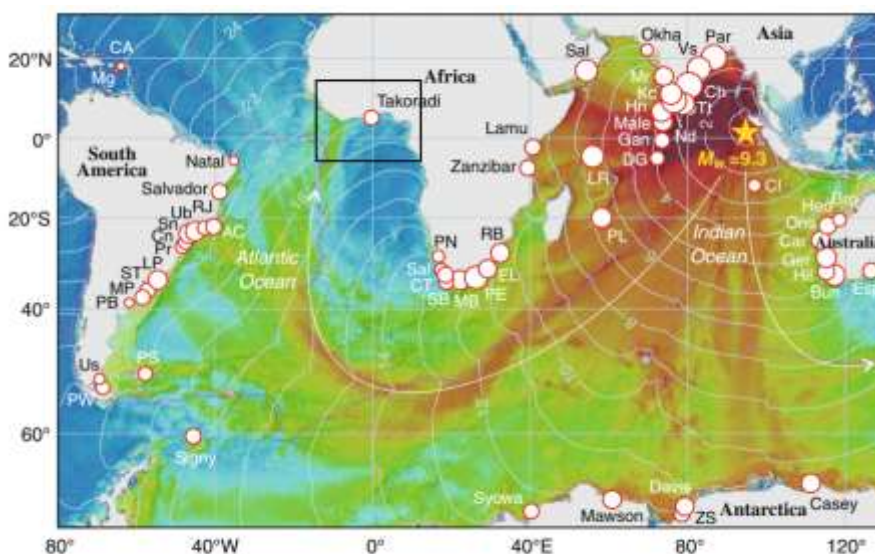


Figure 1 : *Simulated Sumatra tsunami wave heights from its source in Indonesia. Curved with arrows indicate propagation direction of tsunami energy flux (Courtesy [5]). The Gulf of Guinea is located in the bold square*

The global warming and its impacts on natural phenomenon are now more visible and constitute a major concern for the world and particularly for the coastal countries. For example, the increase in global sea level could be amplified by local subsidence from anthropic activities [6]. It is well indicated that sea-level rise and changes in storms and the wave climate are expected to increase the size and magnitude of flooded and eroded coastal areas [7]. These phenomena have many effects on coastal communities, coastal infrastructures, and coastal ecosystems. In December 2004 a severe earthquake of magnitude 9.1 centered in the Indian Ocean off northwest Sumatra triggered the great

Indian Ocean tsunami that killed 233 689 people in 14 adjacent Indian Ocean and few fisher men in the Eastern Africa [8]. In March 2011 an Earthquake in the Pacific Ocean has led to the Fukushima tsunami that destroyed most of the coastal cities in Japan and also led to the most severe nuclear accident since the Chernobyl disaster in 1986. The recrudescence of these tsunami phenomena constitutes more and more a concern for the coastal countries and particularly the poor countries having their potential economy along the coast such as the GG's countries. Even if the GG is located in the Atlantic Ocean which is not bordered by major subduction zones constituting the main source for large tsunamis [9], these tsunamis propagate around the world ocean [5].



Figure 2 : Location of the main infrastructures of the Gulf of Guinea countries. (Courtesy [10])

The main objective of this work is to determine the remote impact of the Indian and Pacific tsunamis in the GG. Three main questions have been investigated: (i) Do the Indian and Pacific Ocean tsunamis have a remote impact in the GG? (ii) What are the time lag between the occurrence of these events respectively in the Indian and the Pacific Oceans and, they arrival in the GG? (iii) How much the sea level varies in the GG under the influence of these tsunamis? The sea level data recorded at different tides gauges in the GG, in the Indian and Pacific Oceans have been analyzed through a spectral analysis to determine indirectly the remote impact of the respective Sumatra and Fukushima tsunamis in the GG.

II - MATERIAL AND METHODS

II-1. GLOSS sea level data

The data used in this study are hourly sea level data from Indian, Pacific and Atlantic Oceans. These data are recorded by different Global Sea Level Observing System (GLOSS) stations (**Figure 3**) in the different countries (**Table 1**). To analyze the influence of the 2004 Sumatra tsunami, data from the city Benoa in Indonesia has been used for the Indian Ocean, while the sea-level data at Takoradi (Ghana) during the year 2004 has been used. For the 2011 Fukushima tsunami, the Chichijima Island in Japan and the Son data of Cameroon have been used.

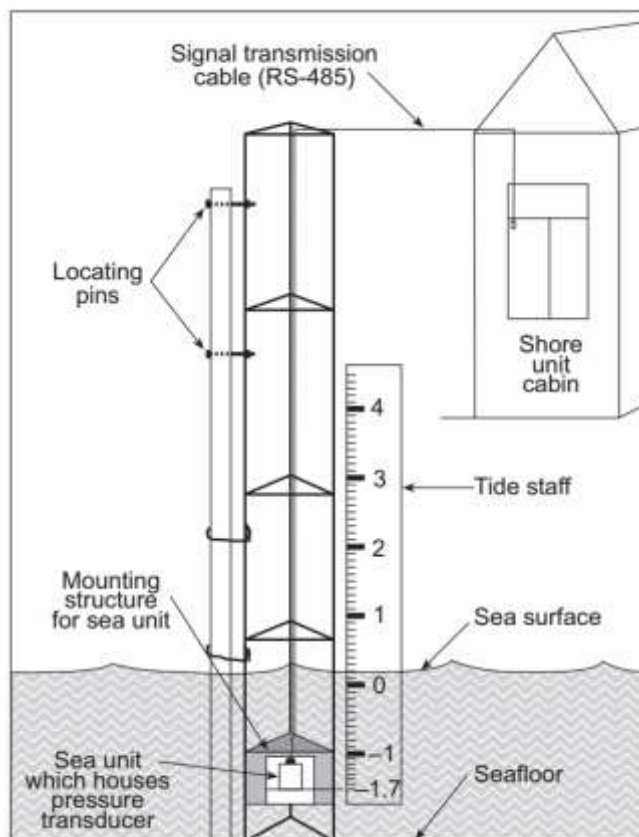


Figure 3 : Coastal sea level measurement station. This equipment constitutes most of the GLOSS stations (Courtesy [4])

Table 1 : *Different stations and their characteristics*

Stations	Country	Ocean	latitude	Longitude
Takorady	Ghana	Atlantic	04.53°N	01.45°W
Son	Cameroon	Atlantic	04.13°N	09.08°E
Benoa	Indonesia	Indian	08.447°S	115.126°E
Chichijima	Japan	Pacific	27.06°N	142.110°E

The different sea levels are characterized by strong diurnal variability with peaks and crest due to the semi-diurnal tides (**Figure 4**). The sea level is higher in the Indian Ocean compared to the GG with highest values reaching 2.5 m at high tides while the minimum values at low tides are similar to the values in the GG (**Figure 4a**). The maxima sea level in the Pacific and in the GG are almost similar. In 2004, we have many missing data compared to 2011 during the months of the respective tsunamis.

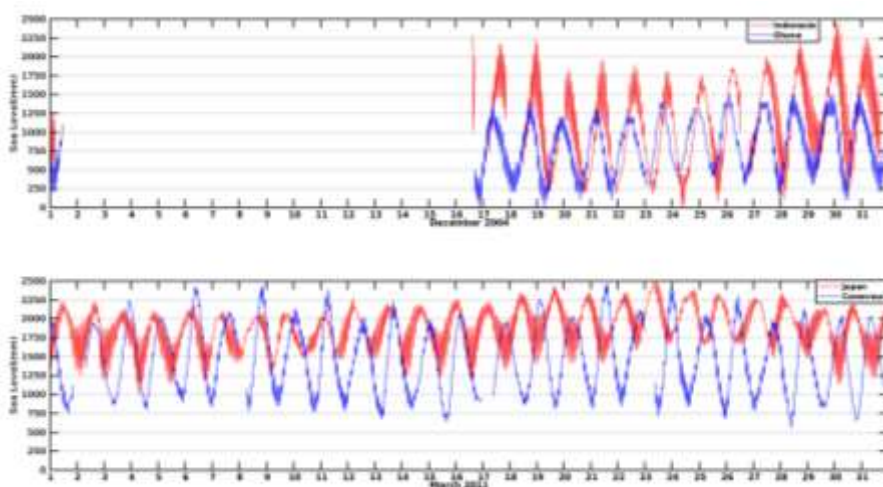


Figure 4 : *Hourly sea level data in the Indian, Atlantic and Pacific Ocean. The data have been represented for the respective tsunami periods*

II-2. Linear Interpolation

The linear interpolation is to approximate data at a point x by a straight line passing through two data points x_j and x_{j+1} closest to x : $g(x) = a_0 + a_1x$ where a_0 and a_1 are coefficients of the linear functions. The percentage of the missing data of Cameroon is very weaker, these missing data have been replaced by linear interpolated data.

II-3. Spectral analysis

The spectral analysis allows to determine the different forces insides the data from their frequencies in the data (**Figure 5**). The frequency or periods of the tsunamis are around 15 mn (**Figure 5**).

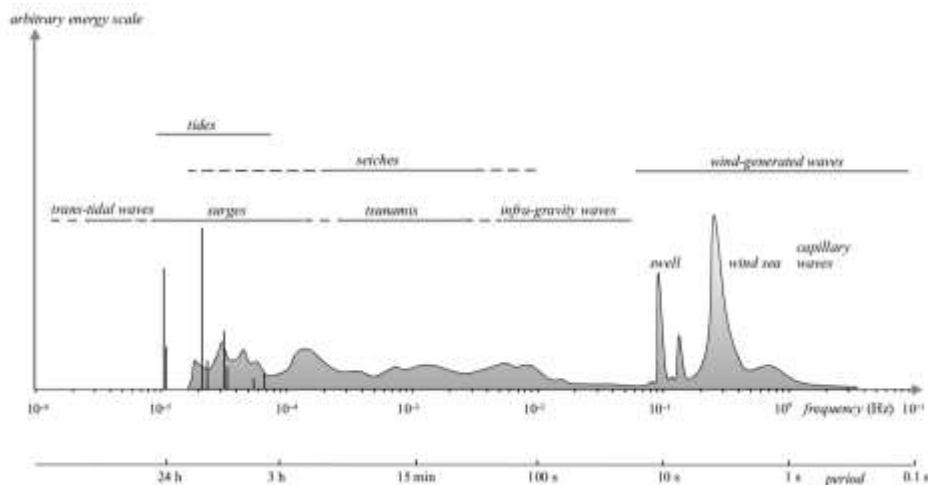


Figure 5 : *Tentative classification of ocean waves according to wave periods. Spectrum and Frequencies of the vertical motions drawing the sea level (Courtesy [11])*

The mathematical development of the Fourier transformation is presented as follow : A function $f(t)$, with a period T , can be decomposed into a summation of simple harmonic terms, which are periodic functions of frequencies that are multiples of the fundamental frequency $1/T$ of the function $f(t)$. Each coefficient in the summation is given by an integral of the product of the function and the complex conjugate of that harmonic term

$$f(t) = \sum_{j=-\infty}^{\infty} g_j e^{-ij\omega t} \tag{1}$$

which is commonly known as the Fourier series. Here $\omega = 2\pi/T$ is the fundamental angular frequency and g_j are the Fourier coefficients, which are given by

$$g_j = \frac{1}{T} \int_0^T f(t) e^{j\omega t} dt \tag{2}$$

The continuous Fourier transform is obtained if the series are restricted to the region of $t \in [-T/2, T/2]$ and then extend the period T to infinity. Let redefine $j\omega \rightarrow \omega$ and $\sum_j \rightarrow (\frac{1}{\sqrt{2\pi}} \int d\omega)$, then the sum becomes an integral

$$f(t) = \frac{1}{\sqrt{2\pi}} \int_{-\infty}^{+\infty} g(\omega) e^{-i\omega t} d\omega \quad (3)$$

which is commonly known as the Fourier integral. The Fourier coefficient is given by

$$g(\omega) = \frac{1}{\sqrt{2\pi}} \int_{-\infty}^{+\infty} f(t) e^{i\omega t} dt \quad (4)$$

The Discrete Fourier Transform (DFT) is usually necessary in the analysis of experimental data, because it is often difficult to establish a clear physical picture just from the raw data taken from an experiment. Let us consider $f(x)$ as a space-dependent physical quantity obtained from experimental measurements. If the measurements are conducted between $x = 0$ and $x = L$, $f(x)$ is non zero only for $x \in [0, L]$. To simplify the problem, let assume that the data are taken at evenly spaced points with each interval $h = \frac{L}{N-1}$, where N is the total number of data points. The data repeat periodically outside the region for $x \in [0, L]$, which is equivalent to imposing the periodic boundary condition in the finite system. The corresponding wavenumber in the momentum space is then discrete too, with an interval $k = 2\pi/L$. The DFT of such a data set can then be expressed in terms of a summation $f_k = \frac{1}{\sqrt{N}} \sum_{j=0}^{N-1} g_j e^{i2\pi jk/N}$, with the Fourier coefficients given by $g_j = \frac{1}{\sqrt{N}} \sum_{k=0}^{N-1} f_k e^{-i2\pi jk/N}$.

The straightforward discrete Fourier transform algorithm is very inefficient because the computing time needed is proportional to N^2 . In order to solve this problem, the Fast Fourier Transform (FFT) approach is used. The FFT algorithm is accomplished with the observation that we can separate the odd and even terms in the discrete Fourier transform as

$$g_j = \sum_{k=0}^{N/2-1} f_{2k} e^{-i2\pi j(2k)/N} + \sum_{k=0}^{N/2-1} f_{2k+1} e^{-i2\pi j(2k+1)/N} \quad (5)$$

What is done is to rewrite the Fourier transform with summation of N terms as two summations, each of $N/2$ terms. The computing time needed for a large set of data point is tremendously reduced.

In this study, a spectral analysis was performed on the hourly data to determine the variability of the data and also to examine the processes which affect the variability of the sea level at the northern coast over short periods (from hourly to diurnal scales). The data have been detrended by removing the total mean from the total time series, allowing us to assume stationary of the data for the power spectra calculation. Since these data are hourly data, i.e., discrete data, a fast Fourier Transform algorithm was used for estimating the periodogram.

The smallest resolvable sampling period (the Nyquist frequency) was 2 hours as we sampled at hourly scale. The frequencies have been computed according to $f'_k = \frac{k}{N\Delta t}$, $k=0, \dots, N$ [12].

II-4. Wavelet analysis

The wavelet transform contains spectral information at different scales and different locations of the data stream, for example, the intensity of a signal around a specific frequency and a specific time. This is in contrast to Fourier analysis, in which a specific transform coefficient contains information about a specific scale or frequency from the entire data space without referring to its relevance to the location in the original data stream. The wavelet method is extremely powerful in the analysis of short time signals, transient data, or complex patterns. A windowed Fourier transform can be formulated to select the information from the data at a specific location. We define

$$g(\omega, \tau) = \frac{1}{\sqrt{2\pi}} \int_{-\infty}^{+\infty} f(t)w(t - \tau)e^{i\omega t} dt \tag{6}$$

as the windowed Fourier transform of the function $f(t)$ under the window function $w(t - \tau)$. The window function $w(t - \tau)$ is used here to extract information about $f(t)$ in the neighborhood of $t = \tau$.

The advantage of the windowed Fourier transform is that it tunes the data with the window function so that we can obtain the local structure of the data or suppress unwanted effects in the data string. However, the Fourier transform treats the whole data space uniformly and would not be able to distinguish detailed structures of the data at different scales. The windowed Fourier transform can provide information at a given location in time, but it fails to provide the data with a specific scale at the selected location. We can obtain information about a set of data locally and also at different scales through wavelet analysis. The continuous wavelet transform of a function $f(t)$ is defined through the integral

$$g(\lambda, \tau) = \int_{-\infty}^{+\infty} f(t)u_{\lambda\tau}^*(t)dt \tag{7}$$

where $u_{\lambda\tau}^*(t)$ is the complex conjugate of the wavelet $u_{\lambda\tau} = \frac{1}{\sqrt{|\lambda|}}u(\frac{t-\tau}{\lambda})$, with $\lambda = 0$ being the dilate and τ being the translate of the wavelet transform. The parameters λ and τ are usually chosen to be real, and they select, respectively, the scale and the location of the data stream during the transformation. The function $u(t)$ is the generator of all the wavelets $u_{\lambda\tau}(t)$ and is called the mother wavelet or just the wavelet. A wavelet analysis was also performed on hourly

sea level data in order to determine both the dominant modes of variability and how these modes vary in time [12] allowing to capture the time lag between the occurrence of the tsunamis and their remote impact in the GG. The hourly data have been detrended by removing the best fitted trend line from the original time series. A Morlet wavelet, normalized by the standard deviation is used. The time step of the is set to $\delta t = 1/4$ hour, so the periods are in hours.

II-5. Data Filtering

The impact of the arrival of the tsunami waves on the sea level heights have been estimated in this study through data filtering. The spectral analysis allows determining the frequency range of the tsunamis and the data have been filtered according to these frequencies to estimate the sea level variability. Consider a time series consisting of the sequence $x(t_n), n = 0, 1, \dots, N - 1$ with observations at discrete times $t_n = t_0 + n\Delta t$, Δt is the sampling increment. A digital filter is an algebraic process by which a sequential combination of the input $\{x_n\}$ is systematically converted into a sequential output $\{y_n\}$. For linear filters, the time-domain transformation is accomplished through convolution of the input with the weighting function of the filter.

$$y_n = \sum_{k=-M}^M \omega_k x_{n-k} + \sum_{j=-L}^L g_j y_{n-j}; n = 0, 1, \dots, N - 1 \quad (8)$$

in which M, L are integers and ω_k, g_j are nonzero weighting functions or 'weights'.

The frequency response or the Fourier transform of $y(t_n)$ is

$$Y(\omega) = \sum_{n=-M}^M y_n e^{-i\omega n \Delta t} = \sum_{k=-M}^M \omega_k e^{-i\omega k \Delta t} \sum_{n=-M}^M x_{n-k} e^{-i\omega(n-k)\Delta t} = W(\omega)X(\omega) \quad (9)$$

The function $W(\omega) = \frac{Y(\omega)}{X(\omega)} = \sum_{k=-M}^M \omega_k e^{-i\omega k \Delta t}$ is the frequency response. Once $W(\omega)$ is specified, the weight ω_k are found through the inverse Fourier transform $\omega_k = \sum_{n=-N/2}^{N/2} W(\omega) e^{i\omega k \Delta t}$, with

$\omega = \omega_n = 2\pi n(\Delta t)$; the gain of the filter is $|W(\omega)|$ and the power $P(\omega) = W(\omega)W(-\omega) = |W(\omega)|^2$

In this work, we used also the third order ($n=3$) band-pass Butterworth filter. It is among the most commonly filters used in Oceanography [12]. A band-pass filter (BPF) is a device that passes frequencies within a certain range and rejects (attenuates) frequencies outside that range. The amplitude of an ideal pass-band filter should satisfy :

$$|W(\omega)| = \begin{cases} 1 & \text{for } \omega_{c1} \leq |\omega| \leq \omega_{c2} \\ 0 & \text{otherwise} \end{cases} \quad (10)$$

The Butterworth filter is a type of signal processing filter designed to have a frequency response as flat as possible in the passband. It is also referred to have a maximal flat magnitude filter. It is a recursive filter of transfer function created using a rational function in sines and cosines.

III - RESULTS AND DISCUSSION

The variability of the sea level at a specific location is due to different forces such as waves, swells, tides, seiches, gravity waves and tsunamis [11]. Each physical phenomenon reacts in a specific frequency range determined by the use of spectral analysis on the detrended sea level data. During the year 2004 and specially in December that corresponds to the month when occurred the Sumatra tsunami in Indonesia, highest spectral peaks are observed both in the Indian and Atlantic Ocean sea level data, particularly at Ghana in the GG insides the period ranges of 50min to 2h corresponding to the frequency range of the 2004 tsunami (**Figure 6**). The peak of the amplitude of the variance varies between 0.8 and 9×10^4 mm²/cpm. The frequency range of tsunami is at 10^{-3} Hz order, i.e 15mn period [11]. To the signal of the tsunami, are observed also seiche and gravity wave signal (**Figure 5**).

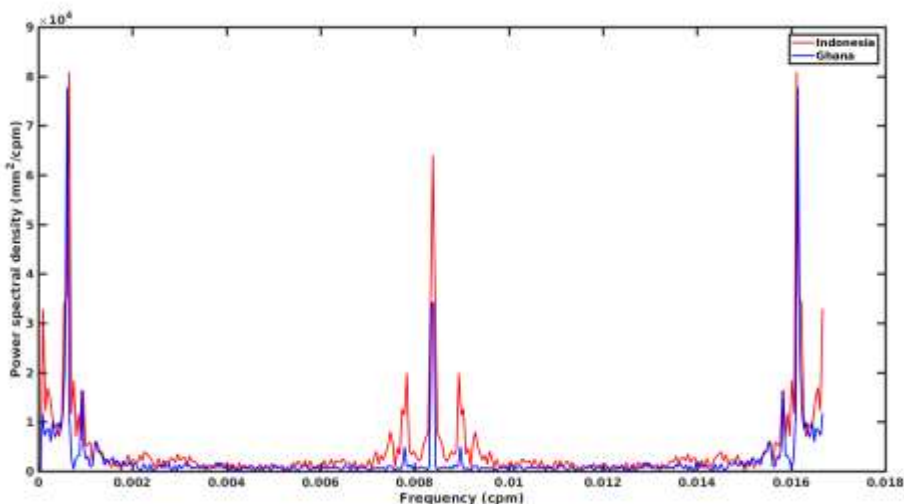


Figure 6a : *Spectrum analysis of the Indian and Gulf of Guinea hourly sea level data. The unit is mm² per cycle per minute (cpm)*

The dominant spectral peaks are observed in the same frequency ranges at the two sites of Takoradi (Ghana) and Benoa (Indonesia) (**Figure 6a**). The first one in the frequency range greater than 2.10^{-3} cpm (8 h 30 min) with greater power spectral density is associated to the surges and tides [11]. In the frequency ranges of [0.01cpm (1 h 40 min) 0.008cpm (2 h)] and [0.018cpm (55 min) 0.016cpm (1h)] are respectively observed the two other dominant spectral peaks (**Figure 6a**). These peaks are both observed in the Indian Ocean and in the GG with the power spectral density greater in the Indian Ocean. These spectral peaks are related to the tsunami source characteristics [4]. In Ghana, the dominant spectral peak is around 45 min [4]. Our data with longer sampling interval of 1h doesn't allow to reach such a precision compared to data with sampling interval of 15min used in [4] and 1min to 3min at other sites [14]. But the spectral peaks with period greater than 1h are also observed in the Indian, Pacific and Atlantic Oceans confirming our results [4, 15]. The spectral peaks corresponding to the period range of 30-60min is probably the most interesting ones because of being the most common for the December 2004 Sumatra tsunami [4, 15, 16].

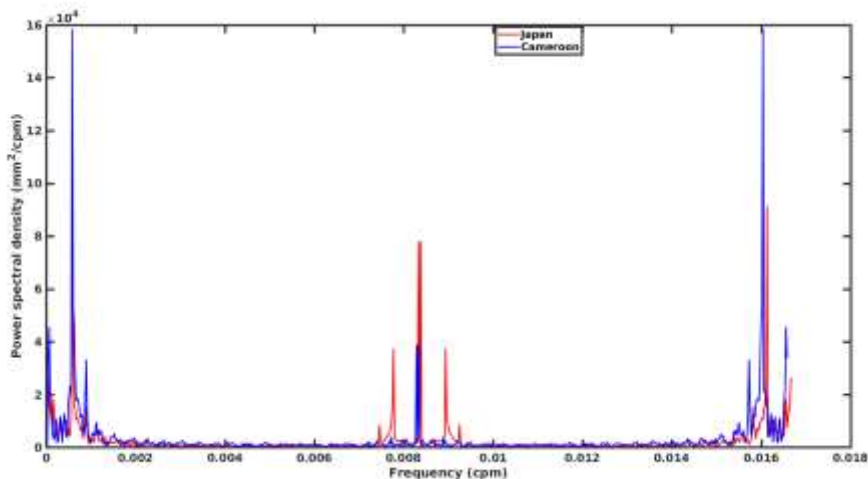


Figure 6b : Spectrum analysis of the Pacific and Gulf of Guinea hourly sea level data. The unit is mm^2 per cycle per minute (cpm)

The Fukushima Tsunamis happened in the Pacific Ocean in March 2011. Its signal propagates across the different oceans bordering the Pacific Ocean. In the Atlantic Ocean and Particularly in the GG, the GLOSS sea-level station installed at Cameroon detected this signal in the respective frequency range of 1.50h to 2h and 58min-60min corresponding to the same range of frequency observed in the sea level data of the Fukushima station (**Figure 6b**). The power

spectral density is greater in Cameroon data than Japan data (**Figure 6b**). The first dominant spectral peak in the frequency range greater than 500cpm (cycle per month) correspond to the tides and the surges [11] while the two other are associated to the March 2011 Fukushima tsunami. The two dominant tsunami periods on the DART (Deep-ocean Assessment and Reporting of Tsunamis) records in the Pacific Ocean were in the period bands of 35-45 min and 60-75 min [14]. The second period band is similar to the second period band observed in this present study. This suggest the arrival of the signal along the GG coastline. The previous results in this study show that the Indian and Pacific tsunami waves reached the GG. The data of 2011 seem not so much good at Cameroon but allow determining the presence of the Fukushima tsunami in the GG. One of the main concern is time delay between the occurrence of these tsunamis and their propagation in the GG. A wavelet analysis is performed on the different sea level data to determine the arrival time of these tsunami signal in the GG. In fact, the spectral analysis through fast Fourier transformation allows to determine the different peaks in the signal and the frequency range determine the physical phenomenon associated to these spectral peaks [11].

The limitation of the FFT is the time location of this dominant spectral peak that is compensated by the wavelet analysis. Highest energy is observed in the period range of 1h to 2h during the month of December 2004 in the Takoradi sea level data (**Figure 7a**). Especially we observe a core of highest energy between days 26 and 27 that should correspond to peak associated to the arrival of the Sumatra tsunami signal in the GG. Outside this period, the other peaks are the signature of the gravity waves. The sea level data of Indonesia shows peaks energy in the period range of 1h to 2h as observed at Ghana. The interesting peak is observed on December 26th that should correspond to the tsunami signal. The sea level data of the Pacific Ocean and Cameroon are characterized by important power in the frequency ranges of 1h and 2h (**Figure 7b**). On March 11, highest energy observed in the Pacific Ocean is followed by high energy in the GG. As for 2004, we observe high variance during the whole month in the Pacific Ocean. We observe the gravity waves, seiches and also the signal of the tsunami the days after the occurrence of the March 2011 Fukushima tsunami. The dominant presence of high energy during the whole period in the period band of 1h to 2h doesn't allow to have good conclusion about the arrival date of the December 2004 Sumatra and March 2011 Fukushima tsunami signals in the GG.

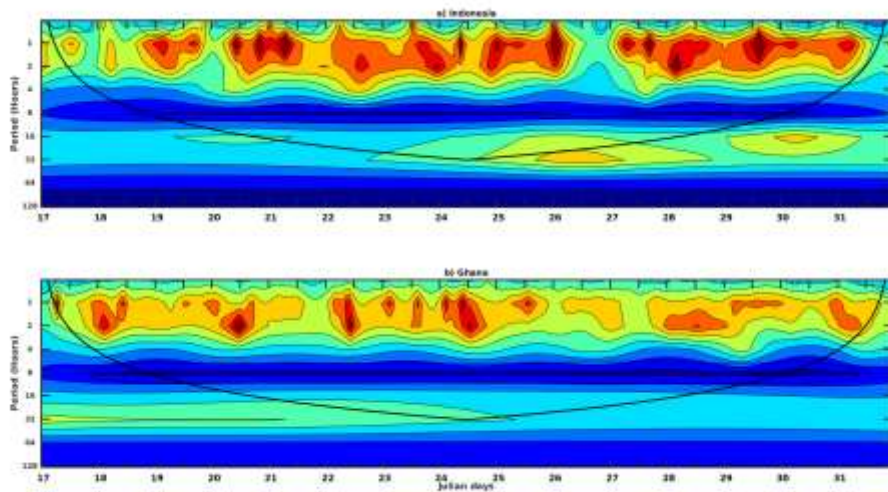


Figure 7a : *Wavelet power spectrum of the sea level data of Indonesia and Ghana. The black contour is the 95 % significance level. Maximum variance corresponding to tide energy has multiplied by -1 to allow the frequency range of 1h to 2h to be more visible. The power spectrum energy is represented in \log_2*

The third main question of this work is to determine how much sea level is changed in the GG by the arrival of the different tsunami waves. The investigation on the two previous questions has shown that the different tsunami waves reached the GG (**Figure 6 and 7**). Their different signals propagate during at least 24 hours to reach the GG and then should contribute to change the sea level in this region. The major change on the sea level in the GG is an increasing of the sea level height as determined by the application of a butterword band pass filter on the GLOSS data of Ghana and Cameroon during the period recording the tsunami signal in the GG (**Figure 8a and 8b**). The FFT filtering method didn't provide encouraging answer and the graphs are not shown, only the butterword filtering method is presented in this section.

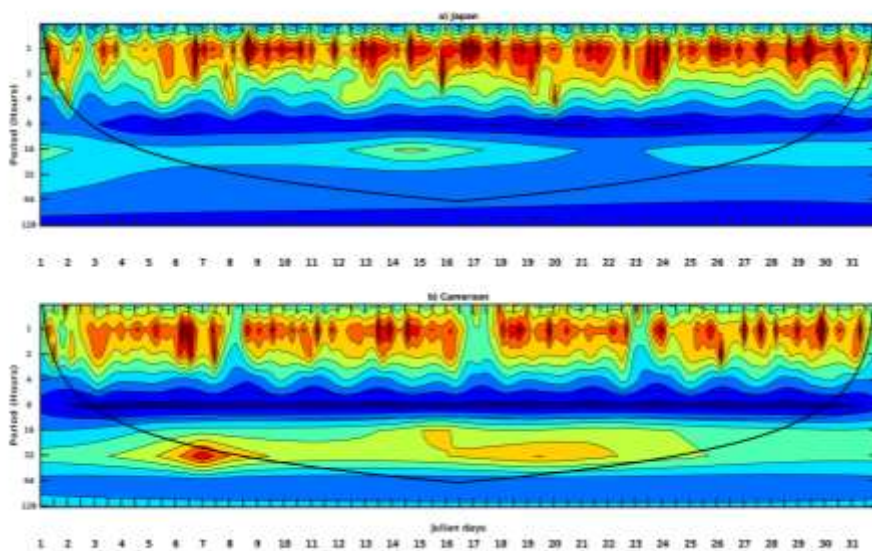


Figure 7b : *Wavelet power spectrum of the sea level data of Japan and Cameroon. The black contour is the 95 % significance level. Maximum variance corresponding to tide energy has multiplied by -1 to allow the frequency range of 1h to 2h to be more visible. The power spectrum energy is represented in log₂*

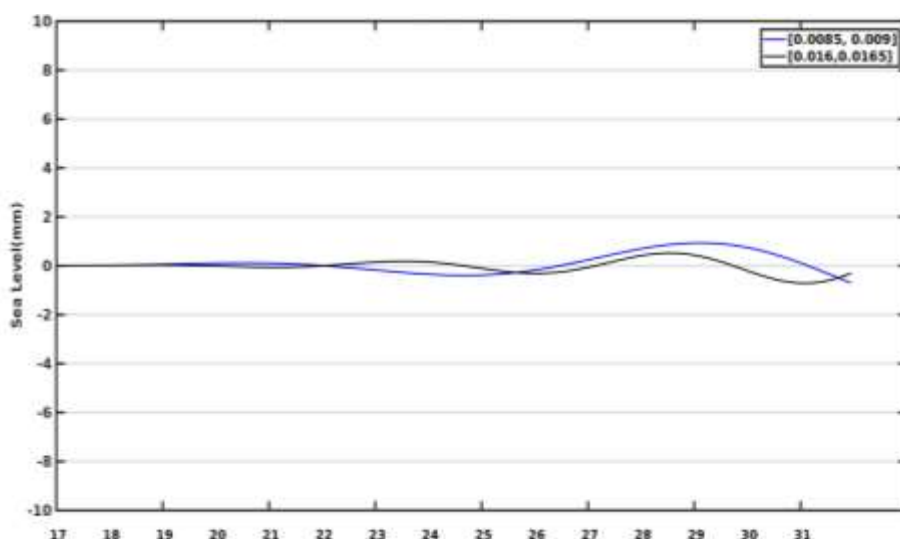


Figure 8a : *Band pass filtering of the sea level data at Takoradi. The different band pass frequencies have been presented in legend*

The remote impact of the Sumatra tsunami in the GG is very weaker with a rise of sea level less than 2 mm (**Figure 8a**) from December 27th, the arrival date of the tsunami at Takoradi [4]. The tsunami waves of frequency range [0.0085cpm 0.009cpm] induces a rise of sea level important than that of frequency range [0.016cpm 0.0165cpm]. They both induce a sea level rise during the period that the tsunami signal washes the GG coastline (**Figure 8a**). On March 11, 2011, the Fukushima tsunami occurred in the Pacific Ocean, and its signal is supposed to reach the GG coastline after at least 1-day modifying therefore the sea level in this region. The band-pass butterword filter applied to the 2011 data of Cameroon shows a rise of the sea level from March 12 to 17 as an impact of this tsunami in this region. The rise of sea level is followed by a decrease during few days and a rise with an amplitude higher than that observed during the 12 to 17 period. The amplitude of the signal is less than 6 mm (**Figure 8b**). For the two tsunamis, their impacts are very weaker in this study compared to the results of [4] who founded an amplitude of 20 cm on December 27-28 at Takoradi.

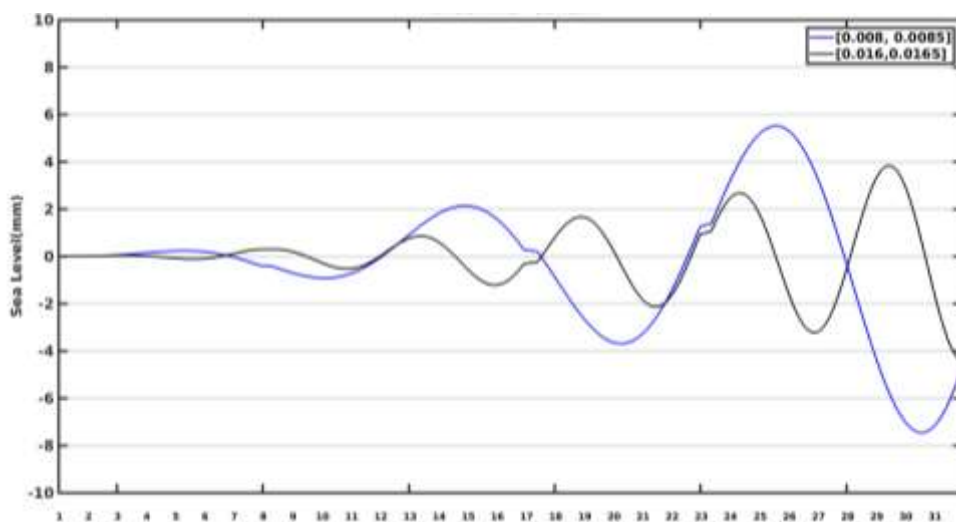


Figure 8b : *Band pass filter of the Cameroun data in the frequency band of the Fukushima tsunamis. The band pass frequencies have been presented in legend*

Because of the long sampling intervals of the data used, it is not possible to efficiently quantify the tsunami wave heights in this study [17]. The data have been averaged to 1h and stored on the GLOSS website. These hourly data filtered already some high frequency variabilities. Most of the studies used sampling interval for the tide gauge of 1mn allowing to easily detect tsunami wave [14].

IV - CONCLUSION

This study uses hourly sea level data from different GLOSS stations located respectively in the Atlantic, Indian and Pacific Ocean to evaluate the remote impact of the 2004 Sumatra and 2011 Fukushima tsunamis along the coastline of the northern GG. The study was entirely based on spectral analysis to identify the variance and associated frequencies of the tsunamis in the sea level recorded at the different stations. The study shows that the signal is dominated by the tides and gravity waves at the different stations. We observe respectively two bands of frequencies concomitantly in the GG and in Indonesia and, in the GG and in the Pacific Ocean corresponding to the frequency ranges of the different tsunamis. These tsunami waves induce a rise of sea level less than 10mm. The wavelet analysis doesn't allow to determine the arrival dates of the different tsunamis along the northern GG coastline because of the strong presence of gravity waves. The weakness of this study is related to the sampling interval of the data which is 1hour where the best sampling rate allowing efficiently analysis of the tsunami is around 1mn to 3mn. Because of the long sampling intervals of the data used, it was not possible to directly quantify exact tsunami wave heights from the spectral filtering. This study shows the need of sea level measurement equipment along the GG's coastline.

ACKNOWLEDGEMENT

The sea level data used in this study are freely available on the GLOSS website. The authors thank the anonymous reviewers for their comments. This work is a capstone project and the first author is grateful to the Master students for their motivation about the discussion concerning this topic.

REFERENCES

- [1] - E. J. ANTHONY, R. ALMAR, M. BESSET, J. REYNS, R. LAIBI, R. RANASINGHE, G.A. ONDOA, M. VACCHI, Response of the Bight of Benin (Gulf of Guinea, West Africa) coastline to anthropogenic and natural forcing, Part 2 : Sources and patterns of sediment supply, sediment cells, and recent shoreline change, *Continental Shelf Research*, 173 (2019) 93 - 103. doi: <https://doi.org/10.1016/j.csr.2018.12.006>
- [2] - E. TOUALY, A. AMAN, P. KOFFI, F. MARIN, T. E. WANGO, Ocean swell variability along the northern coast of the Gulf of Guinea, *African Journal of Marine Science*, 37 (2015) 353 - 361. doi:10.2989/1814232X.2015.107490
- [3] - O. A. DADA, R. ALMAR, M. I. OLADAPO, Recent coastal sea-level variations and flooding events in the Nigerian transgressive mud coast of Gulf of Guinea, *Journal of African Earth Sciences*, 16 (2020) 103668. doi: <https://doi.org/10.1016/j.jafrearsci.2019.103668>
- [4] - A. JOSEPH, J. T ODAMETEY, E. K. NKEBI, A. PEREIRA, R. G. PRABHUDESAI, P. MEHRA, A. B. RABINOVICH, V. KUMAR, S. PRABHUDESAI, P. WOODWORTH, The 26 December 2004 Sumatra tsunami recorded on the coast of West Africa, *African Journal of Marine Science*, 28 (2006) 705 - 712, DOI: 10.2989/18142320609504219
- [5] - V. TITOV, A. B. RABINOVICH, H. MOFJELD, R. E. THOMSON, F. I. GONZALEZ, The global reach of the 26 December 2004 Sumatra tsunami, *Science*, 309 (2005) 2045 - 2048. doi.10.1126/science.1114576
- [6] - R. J. NICHOLLS, Planning for the impacts of sea level rise, *Oceanography*, 24 (2011) 144 - 157. doi:10.5670/oceanog.2011.34
- [7] - M. A. HEMER, J. A. CHURCH, J. R. HUNTER, Waves and climate change on the Australian coast, In : Lemckert, C. (ed.), Proceedings from the International Coastal Symposium (ICS) 2007 (Gold Coast, Australia). *Journal of Coastal Research, Special Issue*, 50 (2007) 432 - 437
- [8] - K. SATAKE, AE. OKAL, J. C. BORRERO, Tsunami and its hazard in the Indian and Pacific oceans : Introduction, *Pure Applied Geophysics*, 164 (2007) 249 - 259
- [9] - V. K. GUSIAKOV, Tsunami history : Recorded, In : The Sea, Tsunamis, A. Robinson, E. Bernard (Eds.), Harvard University Press, Cambridge, USA, 15 (2009) 23 - 53
- [10] - A. AMAN, R. A. TANO, E. TOUALY, F. SILUE, K. A. ADDO, R. FOLORUNSHO, Physical Forcing Induced Coastal Vulnerability along the Gulf of Guinea, *Journal of Environmental Protection*, 10 (2019) 1194 - 1211. <https://doi.org/10.4236/jep.2019.109071>

- [11] - W. H. MUNK, Origin and generation of waves, Proceedings 1st Conference coastal Engineering (Long Beach), New York, ASCE, 1 (1950) 1 - 4
- [12] - W. J. EMERY, R. E. THOMSON, Data Analysis Methods in Physical Oceanography, 2nd and revised edition, *Elsevier, New York*, (2003)
- [13] - C. TORRENCE, G. P. COMPO, A practical guide to wavelet analysis, *Bulletin of the American Meteorological Society*, 79 (1998) 61 - 78
- [14] - M. HEIDARZADEH, K. SATAKE, Waveform and Spectral Analyses of the 2011 Japan Tsunami Records on Tide Gauge and DART Stations Across the Pacific Ocean. *Pure Applied Geophysics*, 170 (2013) 1275 - 1293. DOI 10.1007/s00024-012-0558-5
- [15] - A. B. RABINOVICH, R. E. THOMSON, The 26 December 2004 Sumatra Tsunami : Analysis of Tide Gauge Data from the World Ocean Part 1. Indian Ocean and South Africa, *Pure Applied Geophysics*, 164 (2007) 261 - 308
- [16] - A. B. RABINOVICH, R. E. THOMSON, F. E. STEPHENSON, The Sumatra tsunami of 26 December 2004 as observed in the North Pacific and North Atlantic Oceans, *Surveys Geophysics*, 27 (2006) 647 - 677
- [17] - R. N. CANDELLA, A. B. RABINOVICH, R. E. THOMSON, The 2004 Sumatra tsunami as recorded on the Atlantic coast of South America, *Advances in Geosciences*, 14 (2008) 117 - 128, <https://doi.org/10.5194/adgeo-14-117-2008>